JOURNAL OF CATALYSIS 92, 145–154 (1985)

# *In Situ* X-Ray Diffraction Investigation of the Structural Characteristics of Two Co/ZSM-5 Catalysts

A. G. DHERE AND R. J. DE ANGELIS

*Department of Metallurgical Engineering and Materials Science, University of Kentucky, Lexington, Kentucky 40506*

Received August 1, 1984; revised November 2, 1984

Two Co/ZSM-5 catalysts, one prepared by impregnation with a cobalt nitrate/water media and the other impregnated by cobalt carbonyl, were investigated employing an *in situ* X-ray diffraction chamber mounted on a diffractometer. X-Ray diffraction patterns were obtained following each step in a sequence of processes on each catalyst. The water media-impregnated catalyst displayed the larger particle size and all characteristics remained constant following the initial reduction. The carbonyl-impregnated catalyst showed the formation of a large amount of CoO after exposure to H/CO gas of 1/1 composition at 200°C. Once the CoO formed it would continue to return after subsequent calcining and reduction treatments. 

## INTRODUCTION

The most promising catalysts in the Fisher–Tropsch process are zeolites that offer shape selectivity due to the channel structure. ZSM-5, a zeolite developed by Mobil (*1, 2*), has been very successful in converting alcohol to high-octane gasoline. The crystal structure of ZSM-5 is orthorhombic with lattice parameters of; $a$ = 20.1 Å, $b$ = 19.9 Å and $c$ = 13.4 Å, and the structure contains channels of 5.5 Å diameter.

The addition of metal particles, such as cobalt, to ZSM-5 produces bifunctional catalysts that efficiently convert low $C_2$–$H_4$ compounds to high-octane compounds (*3*). Cobalt has been successfully impregnated onto ZSM-5 from solutions of cobalt nitrate ($Co(NO_3)_2$, $6H_2O$) (*4*) and from cobalt carbonyl vapor, ($Co(CO)_8$) (*5*). The metal particle size has been estimated to be at least three times larger when the nitrate impregnation is employed (*6*). One of the main objectives of this work is to provide a complete structural and morphological description of the metallic cobalt particles and/or cobalt compounds that exist in the catalysts following various thermal treatments in selected environments.

The role of metal carbide and metal oxide phases on catalytic activity and selectivity has been discussed since initially suggested by Fisher and Tropsch (*7, 8*). The carbide and oxide phases are expected to form in Co/ZSM-5 catalysts when the catalyst is exposed to a high-carbon monoxide atmosphere at temperatures about 270°C. Craxford and Rideal (*9*) modeled the formation of hydrocarbons by reaction with hydrogen in the presence of cobalt carbide and cobalt oxide. One objective of this investigation was to attempt to identify the existence of cobalt carbide or cobalt oxide after Co/ZSM-5 catalysts were exposed to carbon monoxide hydrogen gaseous atmospheres.

In addition to the particular cobalt phases possibly controlling activity of the cobalt catalysts it is possible that the structural defects could also be associated with activity. The description of the structural characterization of the metallic cobalt particles is another objective of this investigation.

## MATERIALS AND EXPERIMENTAL

Two cobalt/ZSM-5 catalysts produced at DOE/Pittsburgh Energy Technology Center were employed in this investigation. The catalysts differed in the impregnation



0021-9517/85 $3.00

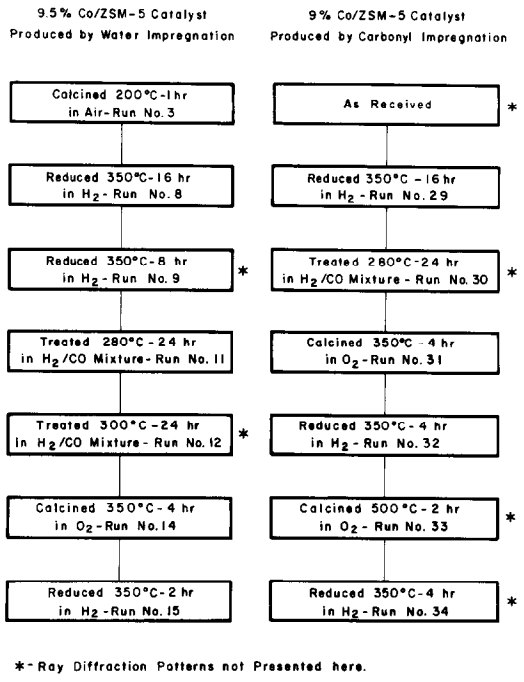


FIG. 1. A processing sequence map showing the "*in situ*" treatments employed for the two catalysts.

method employed. One catalyst was impregnated with 9.5% Co using a cobalt nitrate–water solution (*4*) and 9.0% Co was loaded on the other by cobalt carbonyl vapor impregnation (*5*).

Samples of the catalysts in the powder form were pressed into a disk-shaped die $1\frac{1}{4}$ in. diameter and $\frac{1}{16}$-in. deep which were the specimen holders for the X-ray diffraction camera (vendor—IMIC, 20407 Seaboard Road, Malibu, Calif.) A high-temperature environmentally controlled X-ray camera was employed which was attached to a Picker X-ray Diffractometer. The diffractometer was operated with a nickel tube and was equipped with a curved graphite diffracted beam monochromator. Once a prepared disk catalyst sample was placed in the camera it remained in a controlled environment until the desired sequence of treatments was completed. All thermal and environmental treatments were performed "*in situ*"; therefore, the X-ray beam sampled the same volume of catalyst material throughout all treatments, or runs, on a given sample.

The treatment schedule for each of the two catalysts is shown in Fig. 1. The stages at which X-ray diffraction patterns were collected is also included in Fig. 1.

The X-ray diffraction patterns obtained from the catalysts consisted of superimposed patterns from the crystalline ZSM-5 and the cobalt phases. The ZSM-5 pattern was removed from the pattern of the mixture employing a Fourier technique described previously (*10*). Removal of the ZSM-5 pattern produced a well-defined X-ray pattern of the cobalt containing phases that existed at the particular stages of treatment indicated in Fig. 1. Thus detailed X-ray patterns were obtained from the cobalt phases in the; as received, calcined, reduced, carburized, calcined, and reduced/regenerated states.

## RESULTS

The results obtained from the 9.5% Co/ZSM-5 water-impregnated catalyst will be presented initially. This will be followed by the results obtained on the 9% Co/ZSM-5 carbonyl-impregnated catalyst.

The X-ray diffraction pattern from the cobalt-containing phase obtained after calcining the water-impregnated catalyst in air at 200°C for 1 hr is shown in Fig. 2. The pattern indexed as cobalt oxide $Co_3O_4$. Scherrer analysis of the breadth of the (311) peak at half-maximum intensity gave a $Co_3O_4$ particle size of 35 nm.

The calcined specimen was reduced under flowing hydrogen at 350°C for 16 hr. The X-ray pattern of the cobalt-containing phases is shown in Figs. 3a and b. Two phases exist: hexagonal cobalt metal and a small amount of cobalt oxide (CoO). The Co(100), Co(002), and Co(110) profiles are sharp and the Co(101) profile is very broad. This selective broadening is the type associated with faulting on the basal plane of the hexagonal crystal (*11*). The high concentration of faults explains the absence of the Co(102) profile, which is broadened three

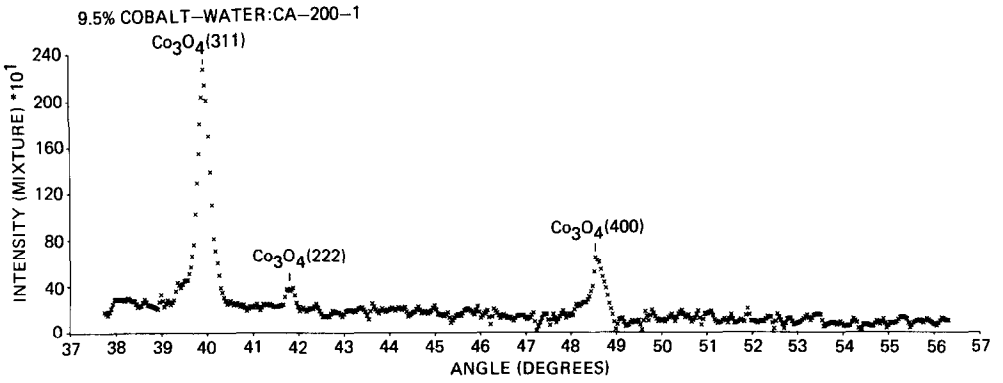


FIG. 2. X-Ray diffraction pattern obtained, after unfolding, from 9.5% Co/ZSM-5 water-impregnated catalyst calcined at 200°C for 1 hr in air. Ni radiation.

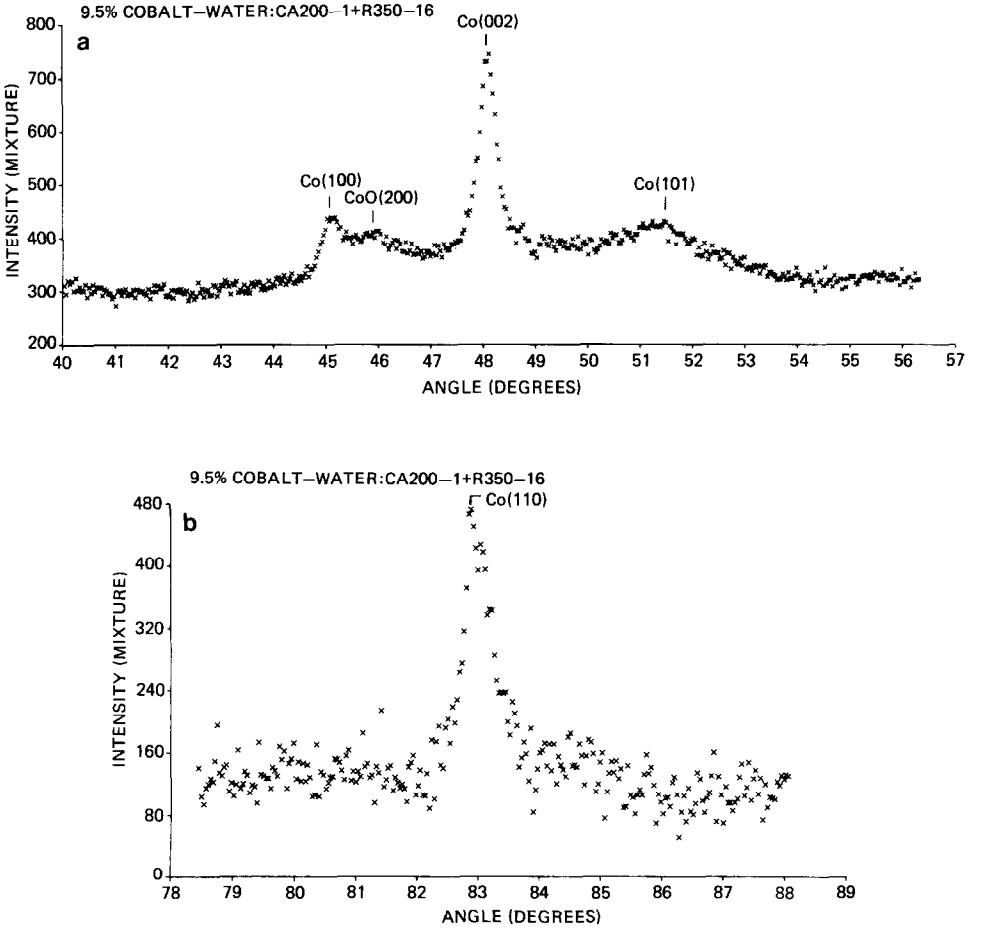


FIG. 3. X-Ray diffraction pattern obtained, after unfolding, from 9.5% Co/ZSM-5 water-impregnated catalyst after calcining and reduction at 350°C for 16 hr in $H_2$. (a) $2\theta$ range 40° to 56°; (b) $2\theta$ range 78° to 88°. Ni radiation.

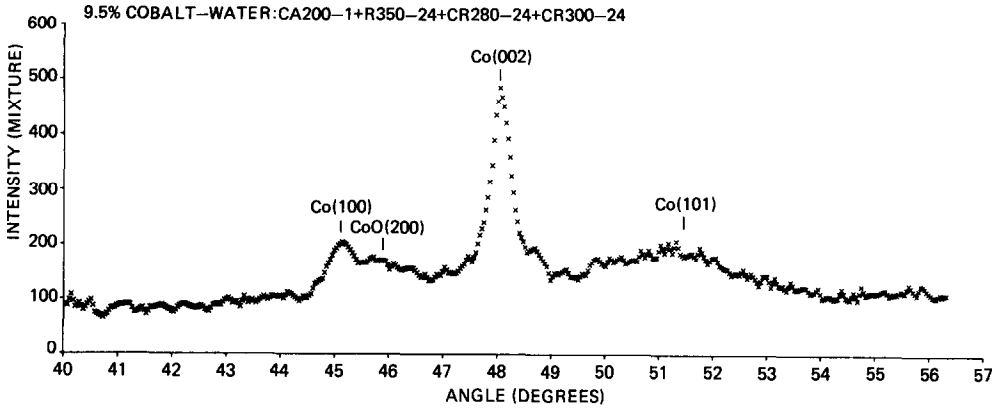


FIG. 4. X-Ray diffraction pattern obtained, after unfolding, from 9.5% Co/ZSM-5 water-impregnated catalyst after calcing, reduction, and carburization at 300°C for 24 hr in 1/1, $H_2$/Co. Ni radiation.

times more than the Co(101) by growth faults (*12*). Growth faults also reduce the intensity of the Co(102) which when combined with the large amount of small particle broadening made the Co(102) nonobservable. An analysis of the extra broadening of the Co(101) observed gave a fault probability of 0.08 (*11, 13*) or on the average every 12th basal plane of cobalt is faulted (*14*).

Following initial reduction the specimen was carburized by exposing the catalyst to a hydrogen–carbon monoxide gas mixture of one to one composition at 280°C for 24 hr, then treated 24 more hours at 300°C in the same atmosphere. There were no new cobalt phases observed after this treatment, the particle sizes of the metallic cobalt remained the same as did the amount of cobalt oxide phase (see Fig. 4). There were no indications in the diffraction pattern of any cobalt phases containing carbon.

Following carburization the catalyst was calcined at 350°C for 4 hr under flowing oxygen. This treatment returned all of the metallic cobalt to $Co_3O_4$ with a diffracting particle size of 10 nm as measured from the half breadth of the (311) line. This pattern is shown in Fig. 5. Following calcining the catalyst specimen was reduced or regenerated at 350°C for 2 hr under flowing hydrogen. The diffraction pattern obtained after this treatment contained Bragg peaks from metallic cobalt and cobalt oxide (CoO)

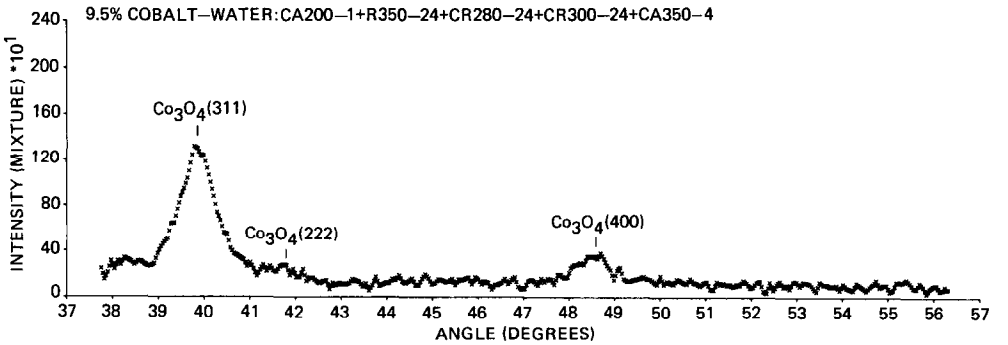


FIG. 5. X-Ray diffraction pattern obtained, after unfolding, from 9.5% Co/ZSM-5 water-impregnated catalyst after calcining, reduction, and carburization, and calcining at 350°C for 4 hr in oxygen. Ni radiation.

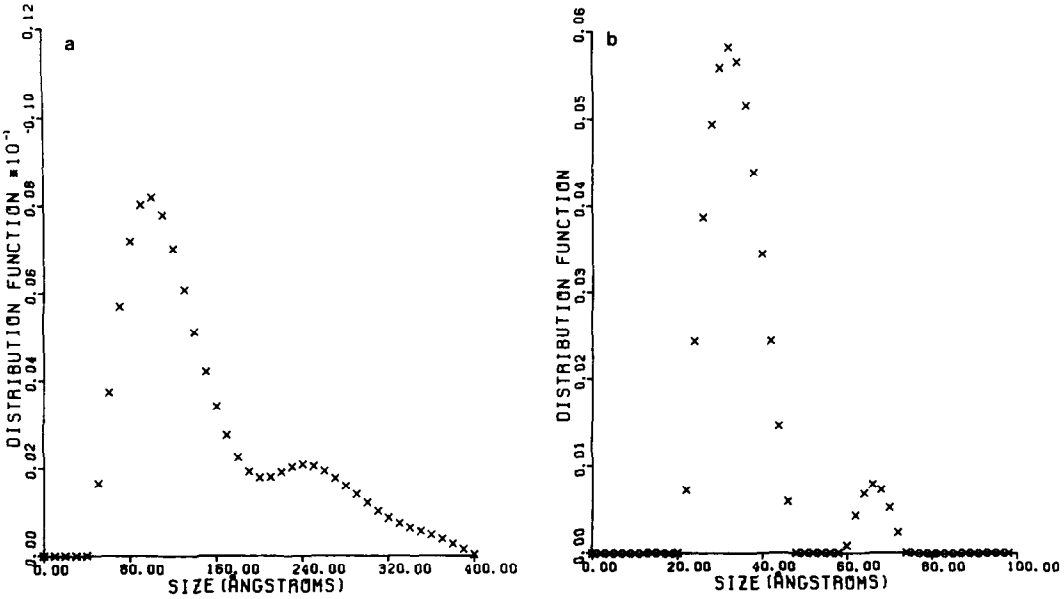


FIG. 6. Particle size distribution functions obtained from single profile analysis of (a) Co(110) and (b) Co(101) profiles recorded in Run No. 8.

phases, identical to Fig. 3. The amounts of these phases and their structural characteristics were essentially the same as observed after the initial reduction.

Particle size distribution functions were obtained from the Co(110) and Co(101) profiles using the method described in Ref. (*13*). The distribution functions shown in Fig. 6 were obtained after the initial reduction treatment. The particle size distribution functions of metallic cobalt obtained at later stages of processing were not significantly different from Fig. 6.

A summary of the observations made from the X-ray diffraction patterns obtained on these specimens is given in Table 1. Notice that the intensity ratio of Co(002) and CoO(200) did not change much during the treatments. The ratio remains constant at a value of about four.

TABLE 1

Summary of X-Ray Diffraction Results Obtained from 9.5% Co/ZSM-5 Catalysts Produced by Impregnation from Water Medium

| Run No. | Treatment | Phases observed/(*hkl*) Particle size | $\frac{I[Co(002)]}{I[CoO(200)]}$ |
|---|---|---|---|
| 3 | 200°C-1 hr-Air | $Co_3O_4$ (311) 35 nm | NA |
| 8 | +Red. 350°C-16 hr-$H_2$ | CoO/no measurement<br>Co/(002) 25 nm; /(101) 3.5 nm; /(110) 17.0 nm | 3.29 |
| 9 | +Red. 350°C-8 hr-$H_2$ | Same as Run No. 8 | NA |
| 11 | +280°C-24 hr-$H_2$/CO | Co/(002) 24 nm; /(110) not measured | 4.0 |
| 12 | +300°C-24 hr-$H_2$/CO | Co/no measurement | 4.0 |
| 14 | +350°C-4 hr-$O_2$ | $Co_3O_4$ (311) 10.0 nm | NA |
| 15 | +350°C-2 hr-$H_2$ | CoO/no measurement<br>Co/(002) 24.0 nm; /(101) 3.8 nm; /(110) 23.0 nm | 3.41 |

*Note.* All metallic cobalt particle sizes were obtained using the single profile technique in Ref. (*13*).

Observations similar to those made on the water-impregnated catalyst were also made on the carbonyl-impregnated catalyst. As carbonyl vapor is deposited and exposed to air, it transforms to the cobalt oxide in a very fine dispersion which was undetectable in the X-ray pattern from the as-received catalyst. The initial observation of cobalt-containing phases were only able to be made after a reduction treatment of 16 hr under flowing hydrogen, at which stage cobalt metal and CoO phases were observed to exist (see Figs. 7a and b). The average diffracting particle sizes of the metallic cobalt calculated from the (002), (101), and (110) profiles were 15, 3.6, and 14 nm, respectively (*13*). The $h - k = 3n$ profiles displayed particle sizes four times larger than the $h - k = 3n \pm 1$ profile indicating the existence of high density of basal plane faulting (*11*). The small amount of cobalt oxide detected was not sufficient to obtain a profile shape from which a particle size measurement could be made.

After reduction the carbonyl catalyst was carburized in one/one, $CO/H_2$, at 280°C for 24 hr. The X-ray diffraction pattern of the cobalt-containing phases, shown in Fig. 8,

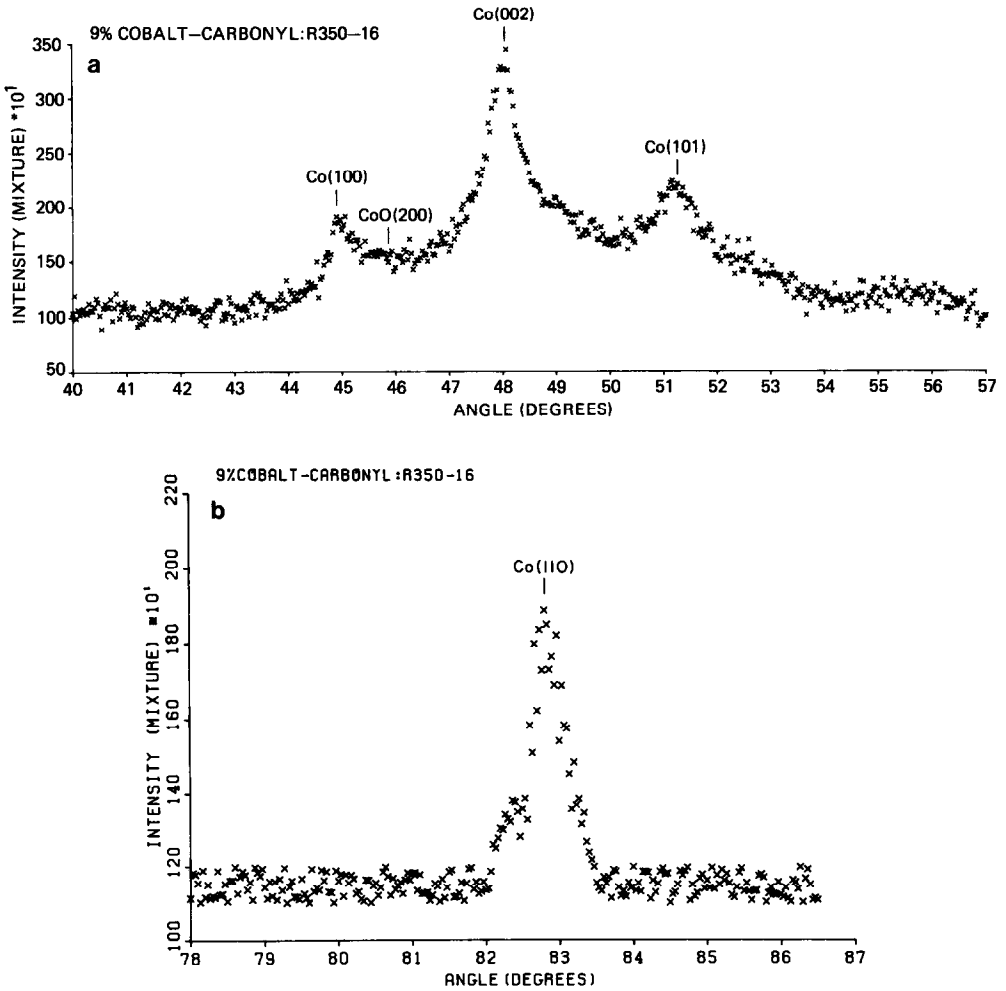


FIG. 7. X-Ray diffraction pattern obtained, after unfolding, from 9% Co/ZSM-5 carbonyl-impregnated catalyst after reduction at 350°C for 16 hr in flowing hydrogen. (a) $2\theta$ range 40° to 57°; (b) $2\theta$ range 78° to 87°. Ni radiation.

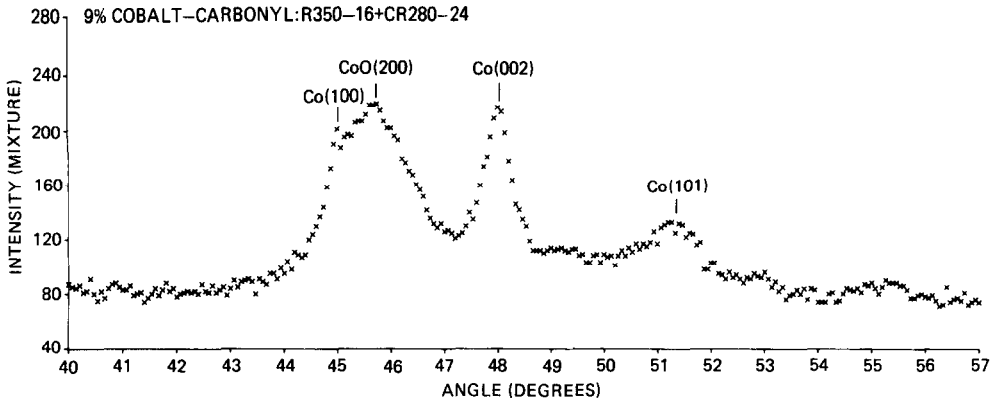


FIG. 8. X-Ray diffraction pattern obtained, after unfolding, from 9% Co/ZSM-5 carbonyl-impregnated catalyst after reduction and carburization at 280°C for 24 hr in 1/1, $H_2$/CO. Ni radiation.

differs from the reduced pattern due to the significant increase in the intensity of the CoO (200) profile. The intensity of the CoO (200) went from just detectable in the reduced sample to the strongest peak after carburization. (Recall the same volume of material is being sampled throughout the experimentation.) The average particle sizes measured from the metallic cobalt peaks were the same as in the reduced condition, the CoO (220) peak (not shown in Fig. 7) half breadth gave particle size of 7 nm.

The carburized sample was calcined in oxygen at 350°C for 4 hr producing complete transformation to $Co_3O_4$ as the diffraction pattern in Fig. 9 indicates. The average particle size of the $Co_3O_4$ calculated from the (311) profile half breadth was 16 nm, about the same size as metallic cobalt particles observed in the reduced and carburized conditions. The calcined catalyst was regenerated by exposure to hydrogen at 350°C for 4 hr. The X-ray pattern observed at this treatment stage was identical to Fig. 8. The amounts and particle sizes of the metallic cobalt and CoO phases present at this stage of treatment is about the same as observed after carburization. An additional 500°C–2 hr calcining and 350°C–4 hr regeneration cycle was performed on this catalyst specimen and the observed pat-

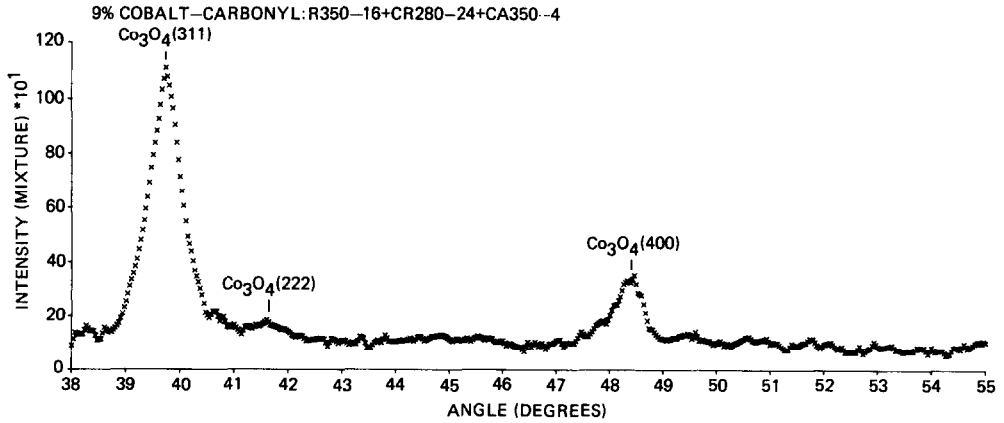


FIG. 9. X-Ray diffraction pattern obtained, after unfolding, from 9% Co/ZSM-5 carbonyl-impregnated catalyst after reduction, carburization, and calcining at 350°C for 4 hr in oxygen. Ni radiation.

TABLE 2

Summary of X-Ray Diffraction Results Obtained from 9% Co/ZSM-5 Catalysts Produced by Impregnation from Cobalt Carbonyl

| Run No. | Treatment | Phases observed/(*hkl*) Particle size | $\frac{I[Co(002)]}{I[CoO(200)]}$ |
|---|---|---|---|
| | As received | No detectable cobalt-containing phases | |
| 29 | 350°C-16 hr-$H_2$ | CoO/traces observed, no measurement<br>Co/(002) 15.0 nm; /(101) 3.6 nm; /(110) 14.0 nm | 4.33 |
| 30 | +280°C-24 hr-$H_2$/CO | CoO/(220) 7.0 nm<br>Co/(002) 15.0 nm; /(101) 3.9 nm | 1.06 |
| 31 | +350°C-4 hr-$O_2$ | $Co_3O_4$/(311) 16.0 nm | NA |
| 32 | +350°C-4 hr-$H_2$ | CoO/(220) 7.0 nm<br>Co/(002) 19.0 nm; /(101) 2.9 nm; /(110) 10.0 nm | 1.07 |
| 33 | +500°C-2 hr-$O_2$ | Same as Run No. 31 | NA |
| 34 | +350°C-4 hr-$H_2$ | Same as Run No. 31 | 1.18 |

*Note.* All metallic cobalt particle sizes were obtained using the single profile analysis technique in Ref. (*13*).

terns were identical to those shown in Figs. 9 and 8, respectively. These results indicate that the phases present after the carburization treatment remain stable and reappear upon reduction at 350°C after each calcining. A summary of the X-ray data collected on the carbonyl-impregnated catalyst is presented in Table 2.

The dramatic change in the amount of CoO in the catalyst is reflected in the ratio of the intensity of the Co(002)/CoO(200) at various stages of treatment which are tabulated in Table 2. The ratio drops from 4.3 after the initial reduction of 1.0 after carburization and remained at this level through the subsequent two calcining and reduction cycles.

## DISCUSSION

The unique experimental conditions and data analysis techniques employed in this investigation allow meaningful statements to be made concerning the characteristics of the cobalt-containing phases observed during treatment of the two catalysts.

The average metallic cobalt particle size resulting from water medium-impregnation (25 nm) is almost twice the size observed in the catalyst produced by impregnation from carbonyl vapor (15 nm). Furthermore, the average size of the metallic cobalt obtained after the initial reduction remained constant during subsequent thermal treatments. This lack of thermal sintering indicates that the metallic dispersion was stable at the temperature of 350°C. No significant changes in the particle size distribution functions for cobalt metal were observed as a function of exposure time at 350°C.

The appearance of a relatively large amount of CoO in the carbonyl-impregnated catalysts after carburizing and its constancy in reappearance after subsequent calcining and reduction is a very unexpected result. This observation can be associated with the larger fraction of smaller size particles existing in the carbonyl-impregnated catalyst which are apparently redispersed during the carburizing treatment.

The increased difficulty of reducing cobalt oxide particles can be attributed to interactions between the particles and the support. However, an alternate explanation for the incomplete reduction can be obtained from small particle effects. The activity, $a$, of a particle of radius, $r$, under equilibrium, is given by the Kelvin equation

$$\ln a/a_0 = \frac{2\gamma V_s}{rRT}, \qquad (1)$$

where $a_0$ is the activity of a planar surface, $\gamma$ is the surface energy, $V_s$ is the molar vol-

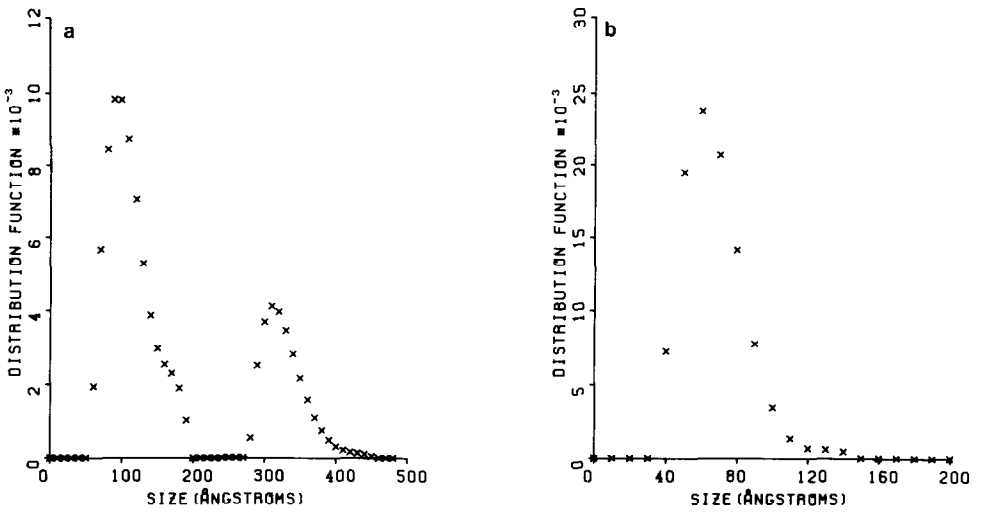


FIG. 10. Particle size distribution functions obtained from single profile analysis of (a) Co(110) and (b) CoO(220) profiles recorded in Run No. 34.

ume, $R$ and $T$ have their usual meanings. Therefore as the radius of the cobalt particle decreases, its activity increases and the equilibrium partial pressure of oxygen or partial pressure ratio of $H_2O/H_2$ reduces. This leads directly to the result that smaller particles are more difficult to reduce.

During the reduction of CoO to Co metal, there is approximately a 75% decrease in volume; therefore, a metallic cobalt particle would be significantly smaller than the CoO particle from which it formed. This effect would, by Eq. (1), increase the activity of the Co particle relative to CoO particle. Thus for a given reduction atmosphere and temperature there would be a particle size of CoO which would be stable while larger particles would reduce to Co.

Support for this explanation can be obtained from the particle size distribution functions of the Co and CoO present in the 9% Co carbonyl impregnated following Run No. 34. These two distributions are shown in Fig. 10. Almost all of the particles of CoO (Fig. 10b) are equal to or smaller than the sizes of particle present as metallic Co (Fig. 10a).

In all conditions investigated for both catalysts the faulting probabilities calculated from the differences in particle sizes measured from the (110) and (101) cobalt profiles, were between 0.06 and 0.08 or on the average 1 out of every 15 basal planes is faulted. This high fault probability places more than $10^{18}$ atoms/g of cobalt in surface positions that their electronic structure is affected by the existence of the faults. These perturbed positions are excellent candidates for active site location and it is possible that the selectivity and activity of the catalysts would be related to the fault character and the density of faulting. Unsuccessful attempts were made to change the fault content by high-temperature annealing at 600°C for 2 to 4 hr. During these attempts to change the fault content of the cobalt it was also observed that the hexagonal phase remained at the annealing temperatures.

At no stage of catalyst treatment was there any diffraction evidence observed for the existence of cobalt carbide. It is recognized that a monolayer or two of carbide on the surface of the cobalt particles would not be detected in the X-ray diffraction spectrum. Therefore, it can only be stated that, if present, cobalt carbide existed in an extremely small crystallite size (<20 Å).

ACKNOWLEDGMENTS

This investigation was sponsored by DOE Contracts DE-AC22-81PC41760 and DE-AS05-82ER12098. One of the authors (A.G.D.) acknowledges STI/MIC of the Brazilian Government for their financial assistance.

REFERENCES

1. Meisel, S. L., McCullough, J. P., Lechthaler, C. H., and Weisz, P. B., *CHEMTECH* **6,** 86 (1976).
2. Chang, C. D., and Silvestri, A. J., *J. Catal.* **47,** 247 (1977).
3. Stencel, J. M., Rao, V. U. S., Diehl, J. R., Rhee, K. H., Dhere, A. G., and De Angelis, R. J., *J. Catal.* **84,** 109 (1983).
4. Obermyer, R. T., Mulay, L. N., Lo, L. C., Oskooie-Tabrizi, M., and Rao, V. U. S., *J. Appl. Phys.* **53,** 2683 (1982).
5. Stencel, J. M., Diehl, J. R., Douglas, L. J., Spitler, C. A., Crawford, J. E., and Melson, G. A., *Colloids and Surfaces* **4,** 331 (1982).
6. Gormley, R. J., Rao, V. U. S., Fauth, D. J., Sprecher, R. F., Pennline, H. W., Youngblood, A. J., and Schehl, R. R., paper presented at 7th North American Meeting of Catal. Soc., Boston, 1981.
7. Fischer, F., and Tropsch, H., *Brennst. Chem.* **7,** 97 (1926).
8. Fischer, F., *Brennst. Chem.* **24,** 489 (1930).
9. Craxford, C. R., and Rideal, E. K., *Trans. Faraday Soc.* **42,** 576 (1946).
10. Dhere, A. G., and De Angelis, R. J., *J. Catal.* **81,** 464 (1983).
11. Houska, C. R., and Averbach, B. L., *Acta Crystallogr.* **11,** 139 (1958).
12. Warren, B. E., "X-Ray Diffraction." Addison–Wesley, New York, 1962.
13. Ganesan, P., Kuo, H. K., Saavedra, A., and De Angelis, R. J., *J. Catal.* **52,** 310 (1978).
14. Dhere, A. G., De Angelis, R. J., Reucroft, P. J., and Bentley, J., *J. Mol. Catal.* **20,** 301 (1983).